Evolutionary-docking targeting bacterial FtsZ

short title: evolutionary FtsZ docking

Coll, J*.
Department of Biotechnology. Centro Nacional INIA-CSIC. Madrid, Spain.

* Corresponding author
Email: juliocollm@gmail.com (JC)
Julio Coll, orcid: 0000-0001-8496-3493

Abstract

To accurately predict binding of inhibitors to the FtsZ cell division protein of the antibiotic-resistance *Staphilococcus aureus* pathogen, evolutionary library docking, ligand-efficiency predictions and rank consensus docking strategies have been sequentially applied. Starting from the crystallographic FtsZ bound model of the PC190723 reference ligand, fragments were derived to generate children molecules fitting low docking-scores with low molecular sizes and hydrophobicities using the DataWarrior Build Evolutionary Library. PC190723 fragment children molecules combined with toxicity filters, and consensus ranks with ligand efficiencies and AutoDockVina docking, identified new benzamide and non-benzamide chemotypes with nanomolar docking-scores and improved specificities to continue with anti-FtsZ ligand investigations.

Keywords: Staphilococcus aureus; FtsZ; docking; interdomain cleft; pharmacophores; evolutionary libraries

Introduction

Bacterial cell division remains under explored for new antibiotics, compared to cell wall synthesis, protein translation or DNA replication.

Bacterial cell division require protein-forming filaments to separate the two daughter cells by a **z**one ring (Z). **F**ilament **t**emperature **s**ensitive **Z**-ring (FtsZ) cell division proteins are the most important component of Z rings and therefore one of the most important antibiotic targets.

Bacterial FtsZ monomers are ~ 300-400 amino acid proteins that contain one molecule each of GTP/GDP nucleotides, Mg^{++} and K^{+} as cofactors. FtsZ filaments are formed by adding non-covalent top-to-bottom adjacent monomers (**Figure 1**). FtsZ filaments are dynamic assembling / disassembling protein polymers constantly exchanging with soluble monomers every ~10 seconds [1]. According to crystallographic, mutational and other studies [2, 3], FtsZ contains two main binding-cavities for known ligands, the **i**nter**d**omain **c**left (idc) and the **n**ucleotide **b**inding **d**omain (nbd). The nbd binds GTP/GDP, and participates in FtsZ folding and GTP γ-phosphate hydrolysis[4]. FtsZ switches from a closed-relaxed conformation in monomers to an open-tense conformation in filaments [5]. Suggested by crystallographic observations[6, 7], the FtsZ transitions were confirmed by several studies[3, 7-9]. At each dimerization step, a new interface is generated including the cocatalytic loop from one of the monomers and the complementary GTP-containing nbd from other monomer.

Experimental screening for bacterial cell division inhibitors among natural extracts and synthetic compounds, identified FtsZ binding ligands with bacterial inhibitory activities at the low μM range[10]. The bacterial inhibition activities of a limited set of ligands correlated better with their idc/nbd binding-affinities than with other experimental assays including inhibition of FtsZ polymerization or regeneration of GTPase activity[10, 11]. Therefore, screening for improved binding to FtsZ may be the best strategy to predict antibacterial activity, as recently suggested [2].

The reference anti-staphylococcal PC190723 inhibitor that binds idc at the FtsZ open-tense conformation at low μM ranges [12-14] was identified by *in vitro* assaying benzamide derivatives [15, 12, 16]. PC190723 contains a difluorobenzamide moiety bound to diheterorings. PC190723 stabilizes the FtsZ filament as suggested by the cocrystalized structure[17, 18]. at low μM ranges However, neither PC190723 nor its varied benzamide analogs became clinically used in medicine, because of pharmacological problems, the generation of bacterial FtsZ gene resistant mutations[9, 19], and despite been tested in combination with other drugs with some success [20]. The PC190723-derived TXA709, TXA436, TXA541 and TXH9179[21] drugs and prodrugs (Taxis pharmaceuticals, Monmouth Junction, Nj, USA)[22, 23, 15, 16, 24, 25] are actually being developed to overcome some of those difficulties[21]. Those ligands were identified by testing a series of drug-like derivatives (heterorings to reduce LogP, minimal numbers of rotatable bonds, introduction of potential hydrogen donors/acceptors, etc) and addition of pro-drug fragments to their molecular backbones. Iterative designed FtsZ benzamide-based derivatives monitored by fluorescent FtsZ binding assays, identified some related chemotypes that showed similar binding concentration than PC190723. Similarly, many other small molecule inhibitors targeting idc have been reported [23, 26-28], however, with similar inhibition concentration ranges. Most probably the limited volume, the hydrophobicity and the steric constrains of the idc binding-cavity, could explain the similar anti-bacterial inhibitor concentrations of alternative drugs[27].

Cocrystal FtsZ complexes with idc ligands, included similar hydrogen bonds (V^{207}, L^{209}, N^{263}), and main hydrophobic interactions (T^{309},G^{196}) than those observed for FtsZ-PC190723 complexes (i.e.,4dxd). PC190723-resistant bacterial mutations confirmed the importance in binding of some of the amino acid residues mentioned above such as G^{196} and T^{309}. On the other hand, an empty cavity implicating residues M^{226}, I^{228}, Q^{192} and L^{249} extends above and behind the idc [9, 10], similarly to the one described for the Taxol binding site in human ß-tubulin [29, 6, 10] perhaps waiting for yet unexplored ligands[2].

Previous attempts to find new FtsZ idc docking candidates by computational screening of Zinc, MolPort or Mcule libraries containing millions-of compounds, identified ~ 100 new ligands with experimental inhibition of bacterial cell division, but only at low μM ranges[30-32].

The main objective of computational docking is to predict conformational poses of each ligand into the binding-cavity of a targeted protein and accurately ranking them according to their affinity. However, no single docking algorithm predicts the same conformational poses or docking-scores with high accuracy respect to their corresponding binding affinities. Actually, consensus docking may be one of the best, yet limited, approach to increase binding predictions. The first consensus averaging docking-scores by several algorithms, had poor accuracies predicting known benchmarks. Alternative methods using ranks rather than scores outperform the averaged results[33]. Consensus combining conformational pose and ranking approaches from several programs (i.e., AutoDockVina, rDock, AutoDock4, PLANTS) improved their isolated performances [34-37]. Similar consensus have been proposed using exponential consensus and RMSD ranks like DockECR (https://github.com/rochoa85/dockECR)[38], or DockingPie (https://github.com/paiardin/DockingPie)[39]. Those strategies employed different algorithms one-by-one and their results were then pooled into different calculation methods to quantify a consensus parameter. Despite benchmark consensus improvements in docking and conformation accuracies, docking-scores and their ranking remain challenging for large screenings.

On the other hand, during screening selection based only in docking-score rank evaluations, the candidates progressively increased in molecular weight and hydrophobicity, trending to select unspecific leads[40, 41]. Alternative parameters to improve ligand efficiency have been developed throughout the years such a **L**igand **E**fficiency (LE), **L**ipophilic **L**igand **E**fficiency (LLE), **L**igand **E**fficiency **L**ipophilic **P**rize (LELP) and many others [42-45]. Therefore, corrections for the influence of molecular weight/hydrophobicity on ligands should be taken into account during the selection of candidates.

We proposed here a sequential rather than a simultaneous consensus strategy, first using the FtsZ crystallographic small binding-cavity and then the wider grid-dependent docking program AutoDockVina (ADV). The search was first restricted to the binding cavity to best explore large chemical spaces by random generation of children molecular libraries (libraries on automatic demand) and automatic selection by fitting the limits of docking-scores, molecular weight and hydrophobicity (DataWarrior). After filtering the children libraries for toxicity, a consensus docking with AutoDockVina generated a final downsized list of new lead chemotypes. Because such strategy allows a first fitting to the selected docking-cavity for ligands controlling docking to cavity, sizes and hydrophobicity, the ligand efficiency (ligand binding per molecular weight or non-hydrogen compounds) may be maintained or even increased during evolution. The generated children libraries can then be ranked not only by docking-scores but also by ligand efficiency parameters. Additionally, to computationally increase the probabilities of bacterial cell wall penetration, some of the bacterial eNTRY rules for drugs[36-38] were finally applied (i.e., primary amines and globularity).

To explore for new chemotypes derived from the PC190723 reference idc ligand, this work combined Data Warrior (DW) evolutionary library generation with ligand efficiency parameters and AutoDockVina. Rather than screening extra-big libraries of molecules, evolutionary and sequential consensus docking strategies may allow for deeper penetration into the vast chemical space[38, 39].

Computational Methods

FtsZ interdomain cleft (idc) target

The molecular model, corresponding to the open-tense FtsZ complexed with the reference ligand PC190723 coded as 4dxd (**R**esearch **C**ollaboratory for **S**tructural **B**ioinformatics, RCSB, **P**rotein **D**ata **B**ank PDB ID) of *Staphylococcus aureus* was selected for the studies. For docking, this target including their GDP nucleotide and idc cavity were centered around a 45x45x45 Å grid surrounding most of the whole FtsZ molecule.

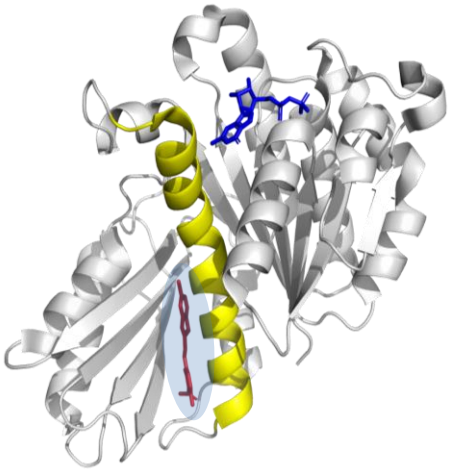

Figure 1
Reference FtsZ 4dxd-PC190723 crystallographic complex cartoon
S.aureus FtsZ crystalized in the presence of the reference FtsZ ligand PC190723.
The antistaphylococcal PC190723 defined the idc binding-cavity .
Yellow, FtsZ central H7 helix (amino acid residues 177-203).
Down blue background, PC190723 4dxd crystallographic idc binding-cavity.
Down red stick, PC190723. Binding to the idc cavity top the diheteroring fragment and to the bottom the difluorobenzamide fragment.
Up blue stick, GDPs at the nbd of the FtsZ

Library of *S.aureus* anti-FtsZ inhibitors

To explore the possibilities of docking algorithms to make real antibacterial predictions, experimentally identified FtsZ inhibitors with **M**inimum **I**nhibitory **C**oncentrations (MIC) data were downloaded from the Chembl database (https://www.ebi.ac.uk/chembl/). MIC records corresponding to *S.aureus* were pooled, manually curated and pooled with previously described UCM inhibitor compounds[10] . A library of 90 experimentally tested compounds with MIC data were expressed in nM.

The DataWarrior docking program

The DataWarrior (DW) docking ("Dock structures into protein cavity") limits its docking exploration to the protein cavity (protein side-chains) supplied as the ligand docked conformer (in this work the crystallographic PC190723), in contrast to the wider grids used by ADV.

The DW last updated version of dw550win.zip was locally downloaded (https://openmolecules.org/datawarrior/download.html). The biweekly last updates including the DataWarrior.exe, jninnchi.jar, mmtf.jar and opsin.jar were periodically substituted at the DW local directory. DW docking uses MMFF94s+ force-field[46] for energy minimization. MMFF94s+ preserved the molecular geometries (double bonds), in contrast to ADV (data not shown). (https://cheminfo.github.io/openchemlib-js/classes/ForceFieldMMFF94.html and https://github.com/cheminfo/openchemlib-js/blob/e88e8a0/types.d.ts#L3334).

The output DW docking-scores were generated in unit-less relative values expanding from -20 to -130. To convert FtsZ DW docking-scores to nM units, the 100-30000 MIC range data obtained from the Chembl bank were converted to nM and then correlated with the unit-less DW docking-scores by polynomial fitting (**Figure S1, red continuous curve**). To obtain ~ MIC nM values for the lower DW docking-scores, the polynomial curve was linearly extrapolated to minimal 1 nM MIC as previously suggested [47] , and to the corresponding minimal -130 DW docking-score observed during our preliminary docking data (**Figure S1, red dashed line**). To estimate their corresponding docking-scores (ds) expressed as ~Kd values, the polynomial and the extrapolated values were exponentially fitted by the formula kd=1507-(1331*EXP(-0.001*ds)). The resulting data were then converted to ΔG energies in Kcal/mol by the formula $\Delta G = 1.4*(\log(Kd*10^9))$. DataWarrior Ligand Efficiency (LE), LLE lipophilic LE and LE lipophilic Price (LELP) parameters were calculated from ΔG taking into account the estimated maximal -1.5 Kcal/mol affinity reported before [48] .

The DataWarrior "Build Evolutionary Library"

The algorithm for generation of children molecules from selected parents included in the DW package was initiated by copy/paste a 2D image of the selected PC190723 parent from a *.sdf file and selection of a *.pdb of the crystallographic PC190723 bound to 4dxd. The PC190723 molecular fragments that will be preserved during evolutionary random modifications were then selected using the lazo tool provided by DW inside the build evolutionary library option. Children molecules were generated by randomly adding small molecular modifications to the parent fragment selected for modification and evolution. Modifications are selected randomly from a list including single atom replacements, insertions, single/double bond changes, atom migrations, ring aromatization/reduction, etc, by the so called Mutator modifications (https://github.com/Actelion/openchemlib/blob/master/src/main/java/com/actelion/research/chem/Mutator.java). Molecular modifications were applied to the parent, then ranked by their fitting criteria and the best fitting molecules used for further modifications in the next generation. After each generation, a calculated weighted sum of all the user selected fitting criteria ranks each children fitness.

Parent-children generations continued automatically until a fitness plateau was reached or stopped by the user after several hours when reaching the ~ 60Gb limits of computer memory. To avoid crashing of runs, the Java heap memory usage was monitored by the Jconsole of Java19 garbage collector (https://download.oracle.com/java/19/latest/jdk-19_windows-x64_bin.msi). The Jconsole garbage collector was manually activated when memory reached high values to maintain the speed of the program.

The fitness criteria and their weight values (wv) applied here as preferences to select for children molecules were minimal docking-scores (wv = 4), molecular weights < than the 355 Daltons of PC190723 (wv= 2), cLog <2 (wv=1), and number of rings <3 (wv= 1). Each generation yielded 128 children molecules of which 8 survived to the next generation (default values). Usually, 50 to 150 generations per parent predicted ~ 0.6 to 1 % fitness to the multiple fitness criteria.

Children generations of ~500 - 2000 new molecules were obtained per parent depending on the parent. The raw children results were filtered by absence of any DW toxic properties including mutagenesis, tumorigenicity, reproductive interference, irritant, and nasty functions. The DW docking-scores were ranked in negative relative units (the more negative, the higher binding).The resulting children molecules were saved as *.dwar files for complete evolutionary data storage and to *.sdf (vs3) files by File/Save Special/SD-File, selecting Docked Protonation: Structure column, Docking pose: Atom coordinates and including Cavity and Natural Ligand, for visualization opening in PyMol and using the PyMol split_states command.

The AutoDockVina docking program

The AutoDockVina (ADV) dockings were performed in Python vs3.8 included in the PyRx098/PyRx1.0 package[46] as described before [49-51] . The protein structure and ligands were first converted to *.pdbqt files by OpenBabel included in PyRx098/PyRx1.0 [52] (https://pyrx.sourceforge.io/). The mmff94s (Merck) force-field energy minimizations, and atom charge calculations to generate individual *.pdbqt files (PyRx-OpenBabel) were chosen for docking [46, 53, 54] . The conservation of geometries were tested by comparing their *InChiKeys* calculated by DataWarrior and/or MolSoft ICM Browser [46, 53-56] .

A 45x45x45 Å grid automatically centered into the target protein surrounding the FtsZ molecule to explore ADV docking-cavity alternatives was chosen, in contrast to DW docking to the PC190723-defined binding cavity. ADV generates rotatable conformers from input ligands and selects the lower docking-scores during iterations [57 ,58] . The conformer predicting the lowest binding-score is selected for output expressing its binding potency as apparent Kcal/mol. Experimental accuracies of ± 2.8 Kcal/mol[59] are predicted for ADV[50] while repetition of ADV docking to the same protein target were < 10 % of docking-scores (n=3-10).

Computational manipulations

DataWarrior (Osiris, vs 5.5.0. Idorsia Pharmaceuticals Ltd, https://openmolecules.org/datawarrior/download.html)[60] and MolSoft (ICM Molbrowser vs3.9-1bWin64bit, https://www.molsoft.com/download.html) were used to visualize and manipulate *.sdf files. The corresponding *in silico* physicochemical and toxicity parameters predicted by DW (mutagenic, tumorigenic, nasty functions, irritant, reproductive effective and nasty functions) were employed post-generation to clean up the children data.

Profiles of DW docking-score ranks and polynomial/exponential fittings were performed with the Origin program (OriginPro 2022, 64 bit, Northampton, MA, USA) (https://www.originlab.com/).

The predicted lead-protein complexes were visualized in PyRx 098/PyRx1.0 (Mayavi), Discover Studio Visualizer v21.1.0.20298 (Dassault Systemes Biovia Corp, 2020, https://discover.3ds.com/discovery-studio-visualizer-download) and PyMOL 2.5.3 (https://www.pymol.org/).

All work was performed in multithreading multi-core i9 (47 CPU) PCSpecialist computer (AMD Ryzen Threadripper 3960X) provided with 64 Gb of RAM (Corsair Vengeance DDR4 at 3200 MHz, 4 x 16 GB) (https://www.pcspecialist.es/).

Results

The reference PC190723 ligand docked to the FtsZ 4dxd crystallographic model was selected to study molecular evolution by the "Build Evolutionary Library" of the Data Warrior program.

According to preliminary observations, to obtain children with lower docking-scores, fragments of PC190723 rather than the whole molecule generated better values when used as parents. Therefore, PC190723 was computationally splitted into top diheterering and bottom difluorobenzamide fragments, to evolve in each case their complementary moieties (**Figure 2**). Once generated, the non-toxic children were extracted from the data and selected to further analysis (non-toxic children varied from 32.9 to 55.7 %, **Table S1**). Most of the children reduced their docking-scores compared to their PC190723 parent. Evolving all PC190723 atoms during evolution generated only slightly lower binding-score profiles, despite a high number of evolved children (**Figure 2, DW25 red**). In contrast, evolving PC190723 fragments showed that children minimal docking-score profiles were similarly predicted when varying their diheterorings **(Figure 2, DW22)** or varying their difluorobenzamide (**Figure 2, DW23**). Evolving the diheterorings of the lowest **DW23** lead parent, predicted ~10-fold lower docking-score profiles, but their molecular sizes and hydrophobicities were higher (unspecific docking), therefore those children were discarded for further analysis (not shown).

Because the tendency of binding-scores to decrease with increasing molecular size and hydrophobicity, the LELP ligand efficiency[47] was calculated from the predicted ΔG values to normalize the docking-scores with respect to the number of non-hydrogen atoms (molecular weight) and logP lipophilicity (hydrophobicity) The graphic comparison between LELP values of children *versus* their DW docking-score rankings predicted ligands below the average LELP of the parent PC190723 (the closest to 0, the higher efficiency). Those children ligands maintaining their DW docking-scores below < 30 nM and LELP below 3.5 were selected as leads for further analysis (**Figure 3A,** gray rectangle).

Similarly, the graphic comparison between ADV docking-scores of children *versus* DW docking-score rankings predicted ligands below the minimal ADV docking-scores predicted by PC190723. Those children ligands maintaining their DW docking-scores below < 30 nM and ADV docking-score below 100 mM were selected as ADV leads for further analysis (**Figure 3B,** gray rectangle).

The number of leads common to DW and ADV arbitrarily selected rectangles (DW+ADV leads) were 8 from **DW22** (80-80.0% of the total number into the rectangles) and 3 from **DW23** (37.5-42.8%). No leads from the **DW25** group could be found predicting low values similar to the other 2 groups. The common DW+ADV leads were tabulated with their properties (**Table S1**), their 2D structures drawn (**Figure 4),** their complexes with 4dxd PyMol visualized (**Figure 5)** and their corresponding amino acid surroundings at 4 Å identified by PyMol analysis of their complexes with FtsZ (**Table S2)**.

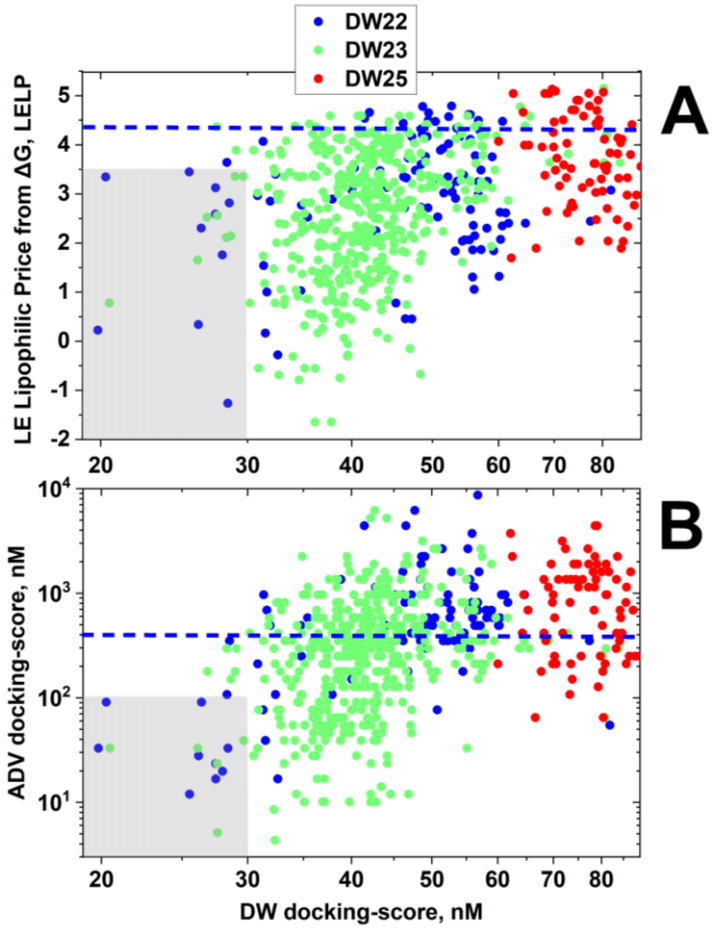

Figure 3
DW docking-score *versus* LELP (A) and ADV (B) of children from PC190723 and fragments
The children molecules were evolved from the parent PC190723 and its fragments (**Figure 2).** The DW and ADV docking-scores were transformed to nM as indicated in methods.
Gray rectangular background, regions selected for consensus
Horizontal dashed blue line, LELP of the PC190723 parent (**A**) and minimal ADV docking-score of PC190723 (**B**)
Blue (DW22), maintaining the bottom difluorobenzamide of PC190723 and evolving the top fragment (R)
Green (DW23), maintaining the top heterorings and evolving the bottom fragment of PC190723 (R)
Red (DW25), evolving the whole PC190723 molecule

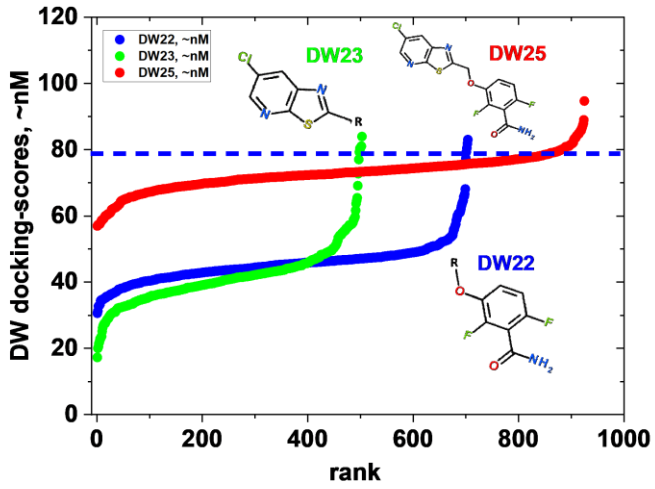

Figure 2
Ranks of evolved children from PC190723, and fragments
The PC190723 2D molecule (upper right in the Figure) was computationally splitted into top diheterorings and bottom difluorobenzamide fragments for independent evolution. Top and bottom names were chosen as suggested by their relative position within the FtsZ idc cavity. Both the crystallographic 4dxd-PC190723.pdb FtsZ complex defining the targeted Protein_Cavity and the PC190723.sdf defining the 2D ligand were uploaded to the DW DW "Build Evolutionary Library" program.
Horizontal dashed blue line, DW docking-score of the PC190723 reference ligand.
Blue (DW22), maintaining the bottom difluorobenzamide and evolving the top fragment (R)
Green (DW23), maintaining the top heterorings and evolving the bottom fragment (R)
Red (DW25), evolving the whole PC190723 molecule

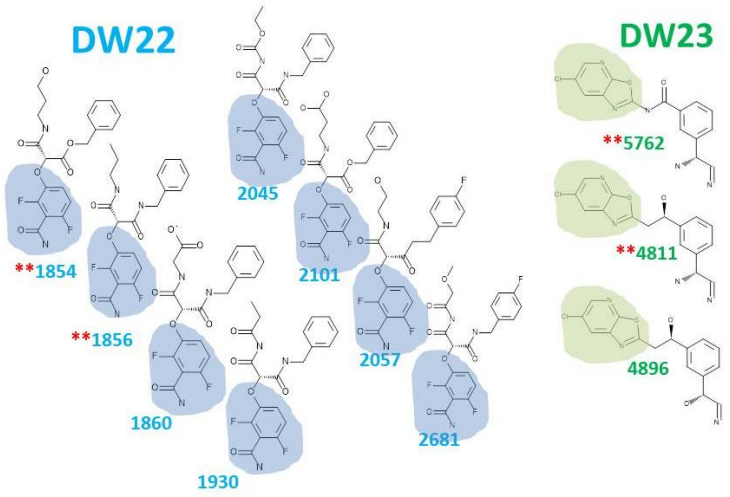

Figure 4
DW+ADV common lead 2D structures
Blue background, difluorobenzamide and oxygen link fragments
Green background, diheterorings fragments
DW22, bottom difluorobenzamide oxygen link plus variable top containing 2 branches and one benzene (**Figure 2**).
DW23, top diheterorings plus variable bottom containing one benzene flanked by 3-4 atoms (**Figure 2**)
, common DW+ADV leads predicting more hydrogen bonds than PC190723 (Table S2**)

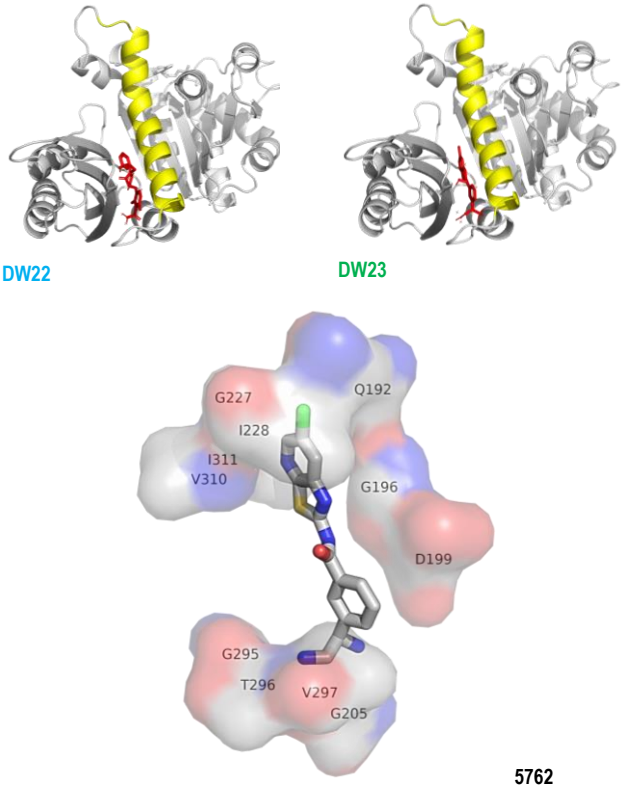

Figure 5
Representative 4dxd mapping of DW+ADV common lead DW22 and DW23 complexes and detailed mapping of the 5762 lead

The 8 DW+ADV common leads (**Figure 3AB**) generated by evolving the top diheterorings of PC190723, predicted one chemotype containing the difluorobenzamide bottom and 2 branches of 3-5 atoms, one of them terminated by a benzene (**Figure 4, DW22**). The 3 DW+ADV common leads generated by evolving the bottom difluorobenzamide of PC190723, predicted a different chemotype containing the top diheterorings and one benzene flanked by 3-4 atoms (**Figure 4, DW23**).

As expected, the common DW+ADV ligands mapped to the PC190723 FtsZ idc binding cavity defined by the crystallographic 4dxd-PC190723 model (**Figure 1 and Figure 5**), except one of the DW22 branches that projected outside of the idc cavity (**Figure 5, DW22**). PyMol visualization of the docked complexes predicted similar docking to a maximum of 26 amino acids expanding a segment between the 192 to 311 residues of FtsZ. Most of the identified amino acids predicted hydrophobic interactions of low specificity. However, higher numbers of the most specific hydrogen bonds than crystallographic PC190723 (4 hydrogen bonds) were predicted for the following leads, 1854 (6 hydrogen bonds), 1856 (6), 4811 (6) and 5762 (9) (**Table S2**). According to all these analysis, the resulting top leader with higher possibilities to bind FtsZ was the 5762 ligand. Both the 5762 and the 4811 leads contained 2 primary amines and predicted a DW globularity of 0.31, lower than the 0.5 threshold proposed by the bacterial eNTRY rules (https://github.com/opensourceantibiotics/murligase/issues/31). Both properties may favor the penetrability of this no-benzamide leads to bacterial cell walls [61-63].

Discussion

Could DW docking-scores, ligand efficiency and consensus ADV docking improve FtsZ binding predictions?

Experimental screening for binding affinity may be a valid strategy to identify antibacterials since inhibition correlated with FtsZ binding affinities better than with either FtsZ polymerization or GTPase assays[10, 11].

However, to predict experimental binding is challenging due to the limitations of present *in silico* docking algorithms, such as DW and ADV. Known limitations include fixing of the docking-cavity amino acid side-chains, eliminating water molecules, unreliable calculation of docking-scores, molecular geometry changes by force-field energy minimizations [53-56], and unreachable chemotype/chemical spaces[38, 39]. Specially the force-field failures to correctly recognize different atom types, would greatly affect the conservation of molecular geometries after minimization[47-50]. Additionally, in the absence of better crystallographic data, the 4dxd crystallographic FtsZ model used here has no K^+, no Mg^{++} and GDP instead of GTP, all of which may not completely reflect the molecular environment for docking. The work described here have also other limitations due to the number of options discarded during screening (i.e., arbitrary selected PC190723 fragments, other multiple fitting criteria, etc). Additionally, known experimental alternatives that could be computationally mimicked to reduce hydrophobicity have not been explored (i.e., benzene mimics[64], non-flat fragment or phosphate additions, amino acid ester or glycerol extensions, and many other known pro-drug alternatives[21]). Furthermore, other FtsZ docking cavities or FtsZ relaxed monomer conformations have not been targeted and possible out-targeting to other proteins has not been tested (i.e, human tubulins and abundant proteins in human serum). Although bacterial FtsZ are structurally similar to eukaryotic tubulins and share their GTPase activities, eukaryotic tubulin ligands do not usually bind FtsZ, and FtsZ ligands do not bind bacterial tubulins, but testing for possible interferences should be included. It may be also expected that during binding, flexibility of the cavity side chains as well as movement of the ligands, could add alternative binding cavities depending of environmental variables (i.e. pH, temperature, ionic concentrations, etc). Although Molecular Dynamic simulations could help to discard or favor some of the complexes, their reliability is still dependent of force-field inaccuracies [65].

Although experimental bacterial inhibitions were proportional to FtsZ bindings, lower docking-score ligands, may not predict higher biological inhibitions. Molecular weight and hydrophobicity may also influence the biological activity, despite a low docking-score. During screening and selection processes based only in docking-score ranks, the candidates increased in molecular weight and hydrophobicity resulting in trends to unspecific leads as demonstrated in many other systems[40, 41]. Among the many parameters proposed to correct for such unspecificities, the LELP parameter was selected here to monitor docking-scores because it reflects in one unique parameter both molecular weight and hydrophobicity unspecificities[42-45]. Ligand efficiency ranks were applied to the lead screening and selection process in the hope to improve their accuracies, but experimental evidence should be performed to validate these efforts.

Since at present no scoring algorithm has proven yet to be reliable for every chemotype, a consensus between at least two different algorithms seem to be necessary to select the many leads generated by explorations of the vast chemotype space[66, 67]. In this work, a minimal consecutive consensus docking by ranks has been introduced using DW and ADV to theoretically increase prediction accuracies, as suggested in other systems[53-56].

Therefore, it may be expected that combining low docking-scores, high ligand efficiencies and consensus docking by ranks, helped to improve binding predictions.

Could evolutionary libraries contribute to expand the exploration of the FtsZ chemotype space?

There are an enormous amount of chemotype possibilities to be computationally explored for FtsZ docking ligands [66, 67]. Despite using the evolutionary docking to explore libraries on-demand applying fitting criteria, only a small percentage of the chemotype space possibilities has been explored here. Some sense of possible future work was experienced when combining multiple fitness criteria values during the design of PC190723 evolutionary libraries. Much large numbers of possible combinations could be generated than those minimally explored here. The DataWarrior parent-children evolutionary algorithm is powerful, specially when including docking as fitting criteria. Nevertheless, including access to other external docking algorithms or iteration of DW runs with identified leads could further increase the DW evolutionary library penetration into the unknown chemotype/chemical space. Developing new evolutionary software introducing not only consensus docking but also screening for reduced docking to out-target proteins (i.e., human tubulins) as new fitting criteria, would automatize the optimization and selection processes. Also the inclusion of new fitting criteria such as toxicity and ligand efficiency (i.e., several toxicity and LE options) would enrich the evolutionary process automatically screening the widest chemical space possible and generating children with increased accuracies.

Because further computational limitations will remain from unexplored physiological environments (i.e., cross-docking to other abundant unknown or similar human proteins, and diverse pharmacological properties), a relatively high number of chemotype alternatives would be desirable to predict to filter out those with undesirable properties. Despite including the maximal number of computational criteria, some of those properties may be difficult or impossible to predict computationally. Experimental confirmation will be always required.

Concluding remarks

Combination of DataWarrior evolutionary docking, ligand efficiency estimations, and ADV consensus docking, identified a few chemotypes predicting low nanomolar docking-score ranges targeting known FtsZ cavities. Additionally, further *in silico* predictions of the viability of chemical synthesis of each out-ligand chemotype may help to filter those candidates before chemical synthesis for experimental assessment. The results remain to be confirmed by new docking algorithms (additional consensus docking) with improved force-fields [53-56], and *in vitro/in vivo* binding to FtsZ before physiological and pharmacological tests.

Supporting information

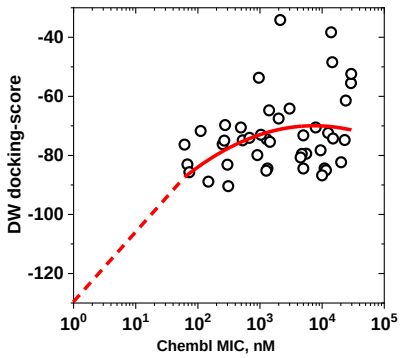

Figure S1
Correlation of anti-FtsZ MIC and DW docking-scores
Compounds with *S.aureus* FtsZ Minimum Inhibitory Concentrations (MIC) were downloaded from ChemDl, enriched with UCM compounds [68], and filtered to <30000 nM before docking. **Red continuous curve**, 9th order polynomial fitting of MIC vs DW docking-scores (Origin) **Red dashed line**, hypothetical extrapolation to minimal -90 to -130 DW docking-scores

Table S1
Resume of molecular properties of the common DW+ADV leads from Figure 4

Number of children	%no toxic	children ID	DW ds	DW nM	ADV nM	MW	nH A	cLogP	LE	LELP
PC190723	-------	----------	-70.4	79.0	500	355	23	2.1	0.4	4.4
DW22		2681	-110.9	19.8	33	453	32	0.1	0.3	0.2
889	> 55.7	**1856	-107.1	25.5	12	405	29	1.3	0.4	3.4
		2101	-106.7	26.2	28	438	31	0.1	0.3	0.3
		1860	-105.2	28.4	33	421	30	-0.5	0.4	-1.3
		2057	-110.7	20.3	91	424	30	1.2	0.4	3.3
		2045	-105.8	27.5	23	435	31	1.1	0.3	3.1
		1930	-105.8	27.5	17	419	30	0.9	0.4	2.6
		**1854	-106.5	26.4	91	422	30	0.8	0.4	2.3
DW23		**4811	-110.5	20.5	33	346	23	0.4	0.5	0.8
1527	>32.9	**5762	-105.7	27.6	5	345	23	1.2	0.5	2.6
		4896	-106.7	26.1	33	347	23	0.8	0.5	1.7

The parent molecules were selected from fragments of PC190723 from Figure 3. Common DW+ADV leads were identified from the rectangle areas of DW22 and DW23 (**Figure 3AB,** gray rectangles).The children lead number were automatically assigned by DW as ordered by their generation during the evolutionary library building. Similar lead structures were tabulated with the same background colors.
, leads predicting more hydrogen bonds than PC190723 (Figure 4**).

Table S2
Amino acid residues around 4 Å of PC190723, and DW+ADV common children

position	Aa	Aa	PC190723	TXH9179	2681	1856**	1860	2101	2057	2045	1930	1854**	4811**	5762**	4896
192	Q	Gln													
193	G	Gly													
*196	G	Gly				H								H	
197	I	Ile													
199	D	Asp													
200	L	Leu		H		H							H	H	H
203	V	Val		H		H	H						H	H	
204	S	Ser													
205	G	Gly	H									H			
207	V	Val	H		H			H	H	H	H	H	H	H	H
208	N	Asn		H		H	H	H					H	H	
209	L	Leu	H		H	H	H		H	H	H	H	H	H	
226	M	Met													
227	G	Gly													
228	I	Ile													
261	L	Leu													
*263	N	Asn	H		H	H		H	H	H		H	H	H	H
265	T	Thr			H		H		H	H					
295	G														
296	T													H	H
297	V	Val									H				
299	N	Asn													
307	V	Val													
*309	T	Thr												H	
310	V	Val										H			
311	I	Ile										H			

Aa, Amino acid residues of FtsZ 4dxd at 4 Å distance of the DW+ADV common leads.
The numbers at the common DW+ADV children columns as in **Table S1**.
, leads predicting more hydrogen bonds than PC190723 (Figure 4**).
Dark red amino acids at the left column approximating the idc bottom subdomain.
Light red, amino acid at the left column approximating the idc top subdomain.
* reported resistant mutants to PC190723 inhibition.
Head yellow background and rectangles, PC190723 4dxd crystallographic model [10] and TXH9179 last reported benzamide derivative [21]. **Head blue background and rectangles,** DW22. **Head green background and rectangles**, DW23
H, predicted hydrogen bonds (yellow, blue and green background colored rectangles).

Funding
The work was carried out without any external financial contribution

Competing interests
The author declares no competing interests

Authors' contributions
JC designed, performed and analyzed the dockings and drafted the manuscript.

Acknowledgements
Thanks are specially due to Dr. T.Sander and J.Wahl of Idorsia Pharmaceuticals Ltd. at Allschwil (Switzerland) for their help during the first steps on the windows version into the Data Warrior Build Evolutionary Library. Thanks are also due to Dr. J.M. Andreu of the CSIC at Madrid (Spain) for the initial bibliography, revision and skeptical commentaries on the manuscript, Dr. A. Villena from the University of Leon (Spain) and to Dr. R. Blasco at CSIC-INIA at Madrid (Spain) for their original view points, criticism, paper information and advices.

References

[1]Anderson, D.E., *et al.* Assembly dynamics of FtsZ rings in Bacillus subtilis and Escherichia coli and effects of FtsZ-regulating proteins.*J Bacteriol.* 2004, 186: 5775-81 http://dx.doi.org/10.1128/JB.186.17.5775-5781.2004.
[2]Andreu, J.M., *et al.* The Search for Antibacterial Inhibitors Targeting Cell Division Protein FtsZ at Its Nucleotide and Allosteric Binding Sites.*Biomedicines.* 2022, 10: http://dx.doi.org/10.3390/biomedicines10081825.
[3]Ruiz, F.M., *et al.* FtsZ filament structures in different nucleotide states reveal the mechanism of assembly dynamics.*PLoS Biol.* 2022, 20: e3001497 http://dx.doi.org/10.1371/journal.pbio.3001497.
[4]Huecas, S., *et al.* Nucleotide-induced folding of cell division protein FtsZ from Staphylococcus aureus.*FEBS J.* 2020, 287: 4048-4067 http://dx.doi.org/10.1111/febs.15235.
[5]Huecas, S., *et al.* Energetics and geometry of FtsZ polymers: nucleated self-assembly of single protofilaments.*Biophys J.* 2008, 94: 1796-806 http://dx.doi.org/10.1529/biophysj.107.115493.
[6]Artola, M., *et al.* The structural assembly switch of cell division protein FtsZ probed with fluorescent allosteric inhibitors.*Chem Sci.* 2017, 8: 1525-1534 http://dx.doi.org/10.1039/c6sc03792e.
[7]Wagstaff, J.M., *et al.* A Polymerization-Associated Structural Switch in FtsZ That Enables Treadmilling of Model Filaments.*mBio.* 2017, 8: http://dx.doi.org/10.1128/mBio.00254-17.
[8]Sharma, A.K., *et al.* A salt bridge mediated resistance mechanism to FtsZ inhibitor PC190723 revealed by a single step cell-based screen..*bioRxiv.* 2022: http://doi.org/10.1101/2022.04.06.487355.
[9]Fujita, J., *et al.* Structural Flexibility of an Inhibitor Overcomes Drug Resistance Mutations in Staphylococcus aureus FtsZ.*ACS Chem Biol.* 2017, 12: 1947-1955 http://dx.doi.org/10.1021/acschembio.7b00323.
[10]Huecas, S., *et al.* Targeting the FtsZ Allosteric Binding Site with a Novel Fluorescence Polarization Screen, Cytological and Structural Approaches for Antibacterial Discovery.*J Med Chem.* 2021, 64: 5730-5745 http://dx.doi.org/10.1021/acs.jmedchem.0c02207.
[11]Artola, M., *et al.* Effective GTP-replacing FtsZ inhibitors and antibacterial mechanism of action.*ACS Chem Biol.* 2015, 10: 834-43 http://dx.doi.org/10.1021/cb500974d.
[12]Tan, C.M., *et al.* Restoring methicillin-resistant Staphylococcus aureus susceptibility to beta-lactam antibiotics.*Sci Transl Med.* 2012, 4: 126ra35 http://dx.doi.org/10.1126/scitranslmed.3003592.
[13]Matsui, T., *et al.* Structural reorganization of the bacterial cell-division protein FtsZ from Staphylococcus aureus.*Acta Crystallogr D Biol Crystallogr.* 2012, 68: 1175-88 http://dx.doi.org/10.1107/S0907444912022640.
[14]Elsen, N.L., *et al.* Mechanism of action of the cell-division inhibitor PC190723: modulation of FtsZ assembly cooperativity.*J Am Chem Soc.* 2012, 134: 12342-5 http://dx.doi.org/10.1021/ja303564a.
[15]Haydon, D.J., *et al.* Creating an antibacterial with in vivo efficacy: synthesis and characterization of potent inhibitors of the bacterial cell division protein FtsZ with improved pharmaceutical properties.*J Med Chem.* 2010, 53: 3927-36 http://dx.doi.org/10.1021/jm9016366.
[16]Haydon, D.J., *et al.* An inhibitor of FtsZ with potent and selective anti-staphylococcal activity.*Science.* 2008, 321: 1673-5 http://dx.doi.org/10.1126/science.1159961.
[17]Andreu, J.M., *et al.* The antibacterial cell division inhibitor PC190723 is an FtsZ polymer-stabilizing agent that induces filament assembly and condensation.*J Biol Chem.* 2010, 285: 14239-46 http://dx.doi.org/10.1074/jbc.M109.094722.
[18]Adams, D.W., *et al.* Multiple effects of benzamide antibiotics on FtsZ function.*Mol Microbiol.* 2011, 80: 68-84 http://dx.doi.org/10.1111/j.1365-2958.2011.07559.x.
[19]Stokes, N.R., *et al.* An improved small-molecule inhibitor of FtsZ with superior in vitro potency, drug-like properties, and in vivo efficacy.*Antimicrob Agents Chemother.* 2013, 57: 317-25 http://dx.doi.org/10.1128/AAC.01580-12.
[20]Kaul, M., *et al.* Combining the FtsZ-Targeting Prodrug TXA709 and the Cephalosporin Cefdinir Confers Synergy and Reduces the Frequency of Resistance in Methicillin-Resistant Staphylococcus aureus.*Antimicrob Agents Chemother.* 2016, 60: 4290-6 http://dx.doi.org/10.1128/AAC.00613-16.
[21]Bryan, E., *et al.* Structural and Antibacterial Characterization of a New Benzamide FtsZ Inhibitor with Superior Bactericidal Activity and In Vivo Efficacy Against Multidrug-Resistant Staphylococcus aureus.*ACS Chem Biol.* 2023: http://dx.doi.org/10.1021/acschembio.2c00934.
[22]Butler, M.S. and Paterson, D.L. Antibiotics in the clinical pipeline in October 2019.*J Antibiot (Tokyo).* 2020, 73: 329-364 http://dx.doi.org/10.1038/s41429-020-0291-8.
[23]Jornada, D.H., *et al.* The Prodrug Approach: A Successful Tool for Improving Drug Solubility.*Molecules.* 2015, 21: 42 http://dx.doi.org/10.3390/molecules21010042.
[24]Czaplewski, L.G., *et al.* Antibacterial alkoxybenzamide inhibitors of the essential bacterial cell division protein FtsZ.*Bioorg Med Chem Lett.* 2009, 19: 524-7 http://dx.doi.org/10.1016/j.bmcl.2008.11.021.
[25]Kaul, M., *et al.* An FtsZ-targeting prodrug with oral antistaphylococcal efficacy in vivo.*Antimicrob Agents Chemother.* 2013, 57: 5860-9 http://dx.doi.org/10.1128/AAC.01016-13.
[26]Silber, N., *et al.* Cell division protein FtsZ: from structure and mechanism to antibiotic target.*Future Microbiol.* 2020, 15: 801-831 http://dx.doi.org/10.2217/fmb-2019-0348.
[27]Casiraghi, A., *et al.* Targeting Bacterial Cell Division: A Binding Site-Centered Approach to the Most Promising Inhibitors of the Essential Protein FtsZ.*Antibiotics (Basel).* 2020, 9: http://dx.doi.org/10.3390/antibiotics9020069.
[28]Han, H., *et al.* Recent progress of bacterial FtsZ inhibitors with a focus on peptides.*FEBS J.* 2021, 288: 1091-1106 http://dx.doi.org/10.1111/febs.15489.
[29]Kellogg, E.H., *et al.* Insights into the Distinct Mechanisms of Action of Taxane and Non-Taxane Microtubule Stabilizers from Cryo-EM Structures.*J Mol Biol.* 2017, 429: 633-646 http://dx.doi.org/10.1016/j.jmb.2017.01.001.
[30]Vergoños-Tomas, A. Inhibidores de la Proteína de División Celular Bacteriana FtsZ Dirigidos al Sitio de Unión del Nucleótido.*Ph.D. Thesis, Autonomous University of Madrid, Madrid, Spain.* 2017: https://repositorio.uam.es/handle/10486/680161?show=full&locale-attribute=en.
[31]Ramirez-Aportela, E. Dinámica de los Filamentos de FtsZ y Búsqueda Racional de Inhibidores Sintéticos con Actividad Antibacteriana.*Ph.D. Thesis, Autonomous University of Madrid, Madrid, Spain.* 2017: https://repositorio.uam.es/handle/10486/677469.
[32]Sun, N., *et al.* Rational design of berberine-based FtsZ inhibitors with broad-spectrum antibacterial activity.*PLoS One.* 2014, 9: e97514 http://dx.doi.org/10.1371/journal.pone.0097514.
[33]Palacio-Rodríguez, K., *et al.* Exponential consensus ranking improves the outcome in docking and receptor ensemble docking.*Sci Rep.* 2019, 9: 5142 http:dx.doi.org/10.1038/s41598-019-41594-3.
[34]Scardino, V., *et al.* Combination of pose and rank consensus in docking-based virtual screening: the best of both worlds.*RSC Adv.* 2021, 11: 35383-35391 http:dx.doi.org/10.1039/d1ra05785e.
[35]Plewczynski, D., *et al.* Can we trust docking results? Evaluation of seven commonly used programs on PDBbind database.*J Comput Chem.* 2011, 32: 742-55 http://dx.doi.org/10.1002/jcc.21643.
[36]Plewczynski, D., *et al.* VoteDock: consensus docking method for prediction of protein-ligand interactions.*J Comput Chem.* 2011, 32: 568-81 http:dx.doi.org/10.1002/jcc.21642.
[37]Blanes-Mira, C., *et al.* Comprehensive Survey of Consensus Docking for High-Throughput Virtual Screening.*Molecules.* 2022, 28: http:dx.doi.org/10.3390/molecules28010175.
[38]Ochoa, R., *et al.* dockECR: Open consensus docking and ranking protocol for virtual screening of small molecules.*J Mol Graph Model.* 2021, 109: 108023 http:dx.doi.org/10.1016/j.jmgm.2021.108023.
[39]Rosignoli, S. and Paiardini, A. DockingPie: a consensus docking plugin for PyMOL.*Bioinformatics.* 2022, 38: 4233-4234 http:dx.doi.org/10.1093/bioinformatics/btac452.
[40]Hopkins, A.L., *et al.* Ligand efficiency: a useful metric for lead selection.*Drug Discov Today.* 2004, 9: 430-1 http://dx.doi.org/10.1016/S1359-6446(04)03069-7.
[41]Cavalluzzi, M.M., *et al.* Ligand efficiency metrics in drug discovery: the pros and cons from a practical perspective.*Expert Opin Drug Discov.* 2017, 12: 1087-1104 http://dx.doi.org/10.1080/17460441.2017.1365056.
[42]Hopkins, A.L., *et al.* The role of ligand efficiency metrics in drug discovery.*Nat Rev Drug Discov.* 2014, 13: 105-21 http://dx.doi.org/10.1038/nrd4163.
[43]Murray, C.W., *et al.* Validity of ligand efficiency metrics.*ACS Med Chem Lett.* 2014, 5: 616-8 http://dx.doi.org/10.1021/ml500146d.
[44]Kenny, P.W. The nature of ligand efficiency.*J Cheminform.* 2019, 11: 8 http://dx.doi.org/10.1186/s13321-019-0330-2.
[45]Garcia-Sosa, A.T., *et al.* Design of multi-binding-site inhibitors, ligand efficiency, and consensus screening of avian influenza H5N1 wild-type neuraminidase and of the oseltamivir-resistant H274Y variant.*J Chem Inf Model.* 2008, 48: 2074-80 http://dx.doi.org/10.1021/ci800242z.
[46]Wahl, J., *et al.* Accuracy evaluation and addition of improved dihedral parameters for the MMFF94s.*J Cheminform.* 2019, 11: 53 http://dx.doi.org/10.1186/s13321-019-0371-6.
[47]Keseru, G.M. and Makara, G.M. The influence of lead discovery strategies on the properties of drug candidates.*Nat Rev Drug Discov.* 2009, 8: 203-12 http://dx.doi.org/10.1038/nrd2796.
[48]Kuntz, I.D., *et al.* The maximal affinity of ligands.*Proc Natl Acad Sci U S A.* 1999, 96: 9997-10002 http://dx.doi.org/10.1073/pnas.96.18.9997.
[49]Coll, J. Star-shaped Triazine-derivatives: would they crosslind SARS-CoV-2 spike helices?*ChemRxiv.* 2021, https://chemrxiv.org/engage/chemrxiv/article-details/6133c1096563696d9d222bbd: http://dx.doi.org/10.33774/chemrxiv-2021-xb6sx-v2.
[50]Lorenzo, M.M., *et al.* Would it be possible to stabilize prefusion SARS-COV-2 spikes with ligands?*ChemRxiv.* 2021: http://dx.doi.org/10.26434/chemrxiv.13453919.v2.
[51]Bermejo-Nogales, A., *et al.* Computational ligands to VKORC1s and CYPs. Could they predict new anticoagulant rodenticides?*BioRxiv.* 2021: http://dx.doi.org/10.1101/2021.01.22.426921.
[52]Dallakyan, S. and Olson, A.J. Small-molecule library screening by docking with PyRx.*Methods Mol Biol.* 2015, 1263: 243-50 http://dx.doi.org/10.1007/978-1-4939-2269-7_19.
[53]Lewis-Atwell, T., *et al.* Comparing the Performances of Force Fields in Conformational Searching of Hydrogen-Bond-Donating Catalysts.*J Org Chem.* 2022, 87: 5703-5712 http://dx.doi.org/10.1021/acs.joc.2c00066.
[54]Loeffler, H.H., *et al.* Reproducibility of Free Energy Calculations across Different Molecular Simulation Software Packages.*J Chem Theory Comput.* 2018, 14: 5567-5582 http://dx.doi.org/10.1021/acs.jctc.8b00544.
[55]Wang, Y., *et al.* End-to-end differentiable construction of molecular mechanics force fields.*Chem Sci.* 2022, 13: 12016-12033 http://dx.doi.org/10.1039/d2sc02739a.
[56]Mobley, D.L., *et al.* Escaping Atom Types in Force Fields Using Direct Chemical Perception.*J Chem Theory Comput.* 2018, 14: 6076-6092 http://dx.doi.org/10.1021/acs.jctc.8b00640.
[57]Morris, G.M., *et al.* AutoDock4 and AutoDockTools4: Automated docking with selective receptor flexibility.*J Comput Chem.* 2009, 30: 2785-91 http://dx.doi.org/10.1002/jcc.21256.
[58]Huey, R., *et al.* A semiempirical free energy force field with charge-based desolvation.*J Comput Chem.* 2007, 28: 1145-52 http://dx.doi.org/10.1002/jcc.20634.
[59]Trott, O. and Olson, A.J. AutoDock Vina: improving the speed and accuracy of docking with a new scoring function, efficient optimization, and multithreading.*J Comput Chem.* 2010, 31: 455-61 http://dx.doi.org/10.1002/jcc.21334.
[60]Sander, T., *et al.* DataWarrior: an open-source program for chemistry aware data visualization and analysis.*J Chem Inf Model.* 2015, 55: 460-73 http://dx.doi.org/10.1021/ci500588j.
[61]Richter, M.F., *et al.* Predictive compound accumulation rules yield a broad-spectrum antibiotic.*Nature.* 2017, 545: 299-304 http://dx.doi.org/10.1038/nature22308.
[62]Richter, M.F. and Hergenrother, P.J. The challenge of converting Gram-positive-only compounds into broad-spectrum antibiotics.*Ann N Y Acad Sci.* 2019, 1435: 18-38 http://dx.doi.org/10.1111/nyas.13598.
[63]Parker, E.N., *et al.* An Iterative Approach Guides Discovery of the FabI Inhibitor Fabimycin, a Late-Stage Antibiotic Candidate with In Vivo Efficacy against Drug-Resistant Gram-Negative Infections.*ACS Cent Sci.* 2022, 8: 1145-1158 http://dx.doi.org/10.1021/acscentsci.2c00598.
[64]Levterov, V.V., *et al.* Water-Soluble Non-Classical Benzene Mimetics.*Angew Chem Int Ed Engl.* 2020, 59: 7161-7167 http://dx.doi.org/10.1002/anie.202000548.
[65]Yunta, M.J.R. Docking and Ligand Binding Affinity: Uses and Pitfalls.*American Journal of Modeling and Optimization.* 2016, 4.3: 74-114
[66]Polishchuk, P.G., *et al.* Estimation of the size of drug-like chemical space based on GDB-17 data.*J Comput Aided Mol Des.* 2013, 27: 675-9 http://dx.doi.org/10.1007/s10822-013-9672-4.
[67]Mroz, A.M., *et al.* Into the Unknown: How Computation Can Help Explore Uncharted Material Space.*J Am Chem Soc.* 2022, 144: 18730-18743 http://dx.doi.org/10.1021/jacs.2c06833.
[68]Araujo-Bazan, L., *et al.* Cytological Profile of Antibacterial FtsZ Inhibitors and Synthetic Peptide MciZ.*Front Microbiol.* 2016, 7: 1558 http://dx.doi.org/10.3389/fmicb.2016.01558.